SDC

PUNCTATE INNER PACHYCHOROIDOPATHY

Demographic and Clinical Features of Inner Choroidal Inflammation in Eyes with Pachychoroid Disease

PRITHVI RAMTOHUL, MD,* K. BAILEY FREUND, MD,*† MAURIZIO BATTAGLIA PARODI, MD,‡§ UGO INTROINI, MD,‡ FRANCESCO BANDELLO, MD,‡§ ELISABETTA MISEROCCHI, MD,‡§ MARIA VITTORIA CICINELLI, MD‡§

Purpose: To perform an unsupervised machine learning clustering of patients with punctate inner choroidopathy (PIC) and provide new insights into the significance of pachychoroid disease features in PIC eyes.

Methods: Retrospective multicenter study, including 102 eyes from 82 patients diagnosed with PIC. Demographics, clinical data, and multimodal imaging, including fundus photography, optical coherence tomography, and indocyanine green angiography, were collected. Clusters of eyes were identified, and multilevel logistic regression analysis was performed to compare between-group differences.

Results: Using 17 clinical features, two distinct clusters of patients with PIC were identified. Cluster 1 patients were characterized by older age, high myopia, myopic maculopathy features, thin choroids, multiple lesions, and a higher likelihood of developing patchy chorioretinal atrophy. Cluster 2 consisted of younger age, emmetropia or low myopia, thick choroids, choroidal vascular hyperpermeability on late-phase indocyanine green angiography, and high prevalence of focal choroidal excavation. These features exhibited significant differences ($P < 0.05$) between the two clusters.

Conclusion: While PIC typically affects young myopic female patients with thin choroids, a subset of patients with PIC exhibits features associated with pachychoroid disease. Considering the potential influence of choroidal venous insufficiency on PIC manifestations and secondary complications, we propose the term "punctate inner pachychoroidopathy" to characterize this distinct subtype of PIC.

RETINA 43:1960–1970, 2023

Punctate inner choroidopathy (PIC)/idiopathic multifocal choroiditis is an inflammatory condition that predominantly affects young, healthy female patients with myopia and thin choroids.[1] The characteristic features of acute PIC lesions include multiple gray-yellow chorioretinal spots corresponding to hypofluorescent lesions on indocyanine green angiography (ICGA) and hyperreflective material splitting the retinal pigment epithelium/Bruch membrane (RPE/BrM) complex on optical coherence tomography (OCT).[2,3] Acute PIC lesions may exhibit transient reversible photoreceptor alterations akin to a multiple evanescent white dot syndrome (MEWDS)–like reaction or secondary MEWDS.[4,5] Regression of active PIC lesions leads to punched-out chorioretinal atrophy, often resembling myopic patchy atrophy.[6] Active PIC has been associated with an increased risk of macular neovascularization (MNV).[7]

The pachychoroid disease spectrum includes a heterogeneous group of disorders characterized by choroidal vascular alterations on multimodal imaging (MMI), including dilated choroidal veins (*pachyveins*), inner choroidal thinning, and increased choroidal thickness on OCT, and choroidal vascular hyperpermeability on late-phase ICGA.[8] Recent investigations involving ultra-widefield ICGA and *en face* OCT of the vortex vein system have suggested choroidal venous insufficiency as a common pathophysiologic pathway.[9] We observed patients with MMI features of pachychoroid disease developing active

inflammatory lesions resembling PIC. Some of these patients also presented with focal choroidal excavation (FCE), an OCT finding previously linked to pachychoroid disease.[10] We hypothesized that these patients might represent a distinct subtype of PIC, characterized by unique demographics, MMI findings, and complications that differ from classic PIC.

In this study, we used an unsupervised machine learning technique to investigate the existence of different clusters of patients with PIC. The identification of distinct clinical patterns can enhance our understanding of the pathophysiology, natural progression, and treatment outcomes of chorioretinal conditions, including PIC. Furthermore, recognizing these atypical patterns could reduce the risk of complications associated with misdiagnosis and delayed treatment.

Methods

This observational cohort study included patients with PIC consecutively seen at two tertiary referral centers, the Vitreous Retina Macula Consultants of New York and the Department of Ophthalmology of the San Raffaele Scientific Institute in Milan, from 2005 to 2023. The Western Institutional Review Board (Olympia, WA) and the San Raffaele Institutional Review Board approved this study and waived written informed consent because of the retrospective, noninterventional design. This report adhered to the tenets of the Declaration of Helsinki and complied with the Health Insurance Portability and Accountability Act.

Eligible patients were identified using the electronic health records codes for "multifocal choroiditis" or "punctate inner choroidopathy." Patients with active PIC lesions documented on OCT at any available visits were included. Active PIC lesions were defined as subretinal isoreflective/hyperreflective material splitting the RPE/BrM complex, RPE/BrM interruption with posterior choroidal hypertransmission, and focal choroidal thickening with loss of the normal choroidal architecture.[11,12] Patients with systemic inflammatory or infectious diseases causing PIC-like lesions (e.g., tuberculosis, histoplasmosis, syphilis, or sarcoidosis) and those with conditions causing choroidal vascular hyperpermeability on ICGA (e.g., choroidal tumors, recent ocular surgery, uncontrolled diabetes, or systemic hypertension) were excluded. Patients without OCT data or those with extensive outer retinal and choroidal atrophy (>2 disk diameters) in the macula at the first visit were also excluded.

All patients had undergone complete ophthalmologic examinations, including measurement of the best-corrected visual acuity using Snellen charts, slit-lamp biomicroscopy, indirect fundus ophthalmoscopy, and multimodal retinal imaging. Color fundus photographs (EIDON AF, Centervue Padova, Italy or Topcon TRC-50IX retinal camera, Topcon Medical Systems, Oakland, NJ or Optos plc, Dunfermline, Scotland), spectral-domain OCT (SD-OCT, Spectralis, Heidelberg Engineering, Heidelberg, Germany), high-resolution SD-OCT prototype (High-Res OCT, Spectralis, Heidelberg Engineering, Heidelberg, Germany), OCT angiography (OCTA, PLEX Elite 9000, Carl Zeiss Meditec, Inc, Dublin, CA), near-infrared reflectance imaging (Spectralis, Heidelberg Engineering, Heidelberg, Germany), fundus autofluorescence imaging (Spectralis HRA, Heidelberg Engineering, Heidelberg, Germany or Optos, plc, Dunfermline, Scotland), fluorescein angiography, and indocyanine green angiography (ICGA, Spectralis HRA, Heidelberg Engineering, Heidelberg, Germany or Optos, plc, Dunfermline, Scotland) were reviewed when available.

Detailed chart reviews were performed, and deidentified demographic and clinical data, including age at PIC diagnosis, sex, and refractive error, were collected.

Multimodal Imaging Evaluation

Two retinal specialists (M.V.C. and P.R.) separately evaluated the MMI at the two centers. Enhanced depth imaging SD-OCT scans were used to manually measure the subfoveal choroidal thickness (SCT) and assess foveal involvement of PIC lesions, the development of patchy chorioretinal atrophy,[13] focal choroidal thinning, and subretinal fibrosis after regression of the PIC lesion.[14] SD-OCT volumes were reviewed for the presence of FCE, defined as a concavity in the

From the *Vitreous Retina Macula Consultants of New York, New York, New York †Department of Ophthalmology, NYU Grossman School of Medicine, New York, New York ‡Department of Ophthalmology, IRCCS San Raffaele Scientific Institute, Milan, Italy; and §School of Medicine, Vita-Salute San Raffaele University, Milan, Italy.

Supported by The Macula Foundation Inc, New York, NY. P. Ramtohul was supported by The Philippe Foundation.

None of the authors have any conflicting interests to disclose.

All the authors contributed to the conception or design of the work, the acquisition, analysis, and interpretation of data, drafting the work, and revising it critically for intellectual content. Each coauthor has seen and agrees with how his or her name is listed.

Supplemental digital content is available for this article. Direct URL citations appear in the printed text and are provided in the HTML and PDF versions of this article on the journal's Web site (www.retinajournal.com).

IntRIS Meeting 2023, Los Angeles.

Reprint requests: Maria Vittoria Cicinelli, MD, Department of Ophthalmology, IRCCS Ospedale San Raffaele, University Vita-Salute, Via Olgettina 60, Milan 20132, Italy; e-mail: cicinelli.mariavittoria@hsr.it

choroid without posterior staphyloma or scleral ectasia, and late-phase ICGA for choroidal vascular hyperpermeability, defined as hyperfluorescent areas associated with dye leakage unrelated to MNV. Color fundus photography was used to assess the number of active PIC lesions (single or multiple lesions), the presence of "chrysanthemum lesions" (gray-yellow central lesion surrounded by satellite pale dots),[15] and the presence of peripheral lesions associated with PIC, including punched-out chorioretinal scars and curvilinear streaks (Schlaegel lines).[16] The grading of ophthalmoscopic features typical of myopic maculopathy, including tessellated fundus, diffuse or patchy chorioretinal atrophy, and lacquer cracks, was performed according to the classification system proposed by Ohno-Matsui et al.[17] The occurrence of MNV or secondary MEWDS was recorded at any of the available visits.

Statistical Analysis

Statistical calculations were performed with the open source programming language R. Descriptive statistics were reported as the mean ± SD or frequency and proportions for continuous or categorical variables, respectively.

First, a principal component analysis (PCA) was used to reduce the dimensionality of the data set, and the Kaiser–Meyer–Olkin test was used to validate PCA as the data reduction method. For PCA, the FactoMineR R package was used,[18] and all the numeric variables were scaled to zero mean and unit variance to make them comparable. Principal components with an eigenvalue (measure of the amount of variation contained by each principal component) >1 were retained. The correlation between each variable and the first two principal components was illustrated by a correlation plot, in which positively correlated variables were shown as arrows in the same circle quadrants and negatively correlated variables were grouped on opposite quadrants. The length of each arrow corresponded to the squared coordinates (cosine squared, $\cos^2$) and was proportional to the variable representation on the principal components.

Then, from the geometric space created in PCA, the patients were divided into clusters using the unsupervised machine learning algorithm k-means (*stats* R package), according to the Euclidean distance between each item and the corresponding centroid of predefined clusters. The optimal number of clusters was determined with the NbClust R package, which provided 30 indices for assessing the number of clusters by varying all combinations of cluster numbers, distance measures, and clustering methods. Venn diagrams illustrated the identified clusters and their overlaps, and the Dunn index was used for internal cluster validation.[1] Missing data were imputed with the ClustImpute R package.

Demographic and clinical characteristics were compared between the identified clusters with a multilevel logistic regression analysis to interpret the effects of influencing factors on cluster definition. The patients' identification number was used as the random intercept to account for simultaneous recording from two eyes of the same patient. *P*-values lower than 0.05 were considered statistically significant.

Results

Demographics and Clinical Data

A total of 102 eyes from 82 patients (mean age 42.0 ± 13.7 years) were included. Nine patients had only one visit available for review, and the average follow-up for the remaining patients was 58 ± 46 months. Most of the included patients were female patients (79.4%) and had myopia (−8.01 ± 5.4 diopters) and a tessellated fundus (67.6%). Foveal involvement was observed in 59.8% of eyes on SD-OCT, and signs suggestive of MNV were present in nearly two-thirds of the eyes (62.7%). Subfoveal choroidal thickness showed considerable variation (from 23 to 470 μm) with a mean of 178 ± 106 μm. Focal choroidal excavation was detected in 19 eyes (18.6%). Table 1 summarizes the demographics and clinical data of all patients with PIC.

Principal Component Analysis and Cluster Definition

Seventeen variables were analyzed using the PCA analysis based on data availability, clinical significance, and previous literature review. The Kaiser–Meyer–Olkin test indicated a good scenario for using PCA as a data reduction technique, with a Kaiser–Meyer–Olkin value of 0.73 for the overall sample. Six principal components with eigenvalues > 1 were identified, explaining 66% of the data variance (see **Figure 1A**, **Supplemental Digital Content 1**, http://links.lww.com/IAE/C52). The first principal component (PC1), which accounted for the highest proportion of variance (26.6%), did not show any original variables with a loading magnitude of 30% or higher (see **Table 1**, **Supplemental Digital Content 2**, http://links.lww.com/IAE/C53). The correlation plot in Figure 1A shows the relationships between the variables used in the PCA analysis.

Table 1. Demographic and Clinical Characteristics of all Patients with PIC

	Overall (N = 102 Eyes)
Age (years)	
Mean (SD)	42.0 (13.7)
Median [min, max]	40.5 [14.0, 77.0]
Sex	
Female	81 (79.4%)
Male	21 (20.6%)
Refraction (diopters)	
Mean (SD)	−8.01 (5.4)
Median [min, max]	−8.00 [−23.0, 2.50]
N/A	3 (2.9%)
Tessellated fundus	
No	33 (32.4%)
Yes	69 (67.6%)
Lacquer cracks	
No	61 (59.8%)
Yes	41 (40.2%)
Number of lesions	
Single	41 (40.2%)
Multiple	61 (59.8%)
Peripheral lesions	
No	59 (57.8%)
Yes	19 (18.6%)
N/A	24 (23.6%)
Foveal involvement	
No	41 (40.2%)
Yes	61 (59.8%)
SCT (μm)	
Mean (SD)	178 (106)
Median [min, max]	157 [23, 470]
MNV	
No	38 (37.3%)
Yes	64 (62.7%)
FCE	
No	83 (81.4%)
Yes	19 (18.6%)
Chrysanthemum lesion	
No	87 (85.3%)
Yes	15 (14.7%)
Secondary MEWDS	
No	74 (72.5%)
Yes	28 (27.5%)
Choroidal vascular hyperpermeability	
No	46 (45.1%)
Yes	18 (17.6%)
N/A	38 (37.3%)
Subretinal fibrosis	
No	62 (60.8%)
Yes	40 (39.2%)
Patchy chorioretinal atrophy after PIC lesion regression	
No	41 (40.2%)
Yes	61 (59.8%)
Choroidal thinning after PIC lesion regression	
No	74 (72.5%)
Yes	28 (27.5%)

N/A, not available.

Clinical Characteristics of Punctate Inner Choroidopathy Clusters

Based on 17 indices, the optimal number of clusters identified was 2 (see **Figure 1B**, **Supplemental Digital Content 1**, http://links.lww.com/IAE/C52). Cluster 1 consisted of 65 eyes (64%) of 52 patients, while cluster 2 included 37 eyes (36%) of 30 patients (Dunn index = 0.32) (Figure 1B). Notably, the clustering was symmetric in all 82 patients. Comparisons of the clinical characteristics between the two clusters are presented in Table 2. Eyes in clusters 1 and 2 significantly differed in age (mean years, 45.5 vs. 35.8 years, *P*-value = 0.02), refractive error (mean diopter, −10.5 vs. −3.89, *P*-value = 0.02), and SCT (mean μm, 120 vs. 281, *P*-value < 0.001). Patients in cluster 1 showed a higher prevalence of multiple lesions in the posterior pole (81.5% vs. 21.6%, *P*-value = 0.04) and a higher rate of patchy chorioretinal atrophy (78.5% vs. 27.0%, *P*-value = 0.04) after regression of PIC lesions. Cluster 1 also exhibited a higher occurrence of myopic maculopathy features, with tessellated fundus and lacquer cracks seen in 95.4% and 61.5% of the eyes, respectively (Figure 2). Choroidal vascular hyperpermeability and chrysanthemum lesions were seen more frequently in cluster 2 (12.3% vs. 43.2%, *P*-value < 0.001, and 1.5% vs. 37.8%, *P*-value < 0.001, respectively) (Figure 3). Focal choroidal excavation was exclusively found in cluster 2 (0% vs. 51.4%) (Figures 4, 5). Although not statistically significant, cluster 2 showed a higher rate of subretinal fibrosis (33.8% vs. 48.6%, *P* = 0.3) after the regression of PIC lesions.

Discussion

Cluster analysis is a valuable method for identifying patterns in large data sets and grouping them based on similarities without prior knowledge of the number or nature of the subgroups. In our study, we used unsupervised machine learning and cluster analysis to identify two distinct clinical clusters among patients with PIC. Patients in one cluster were characterized by older age, highly myopic refractive error, myopic maculopathy features, thin choroids, multiple lesions, and higher tendency to develop patchy chorioretinal atrophy. The other cluster featured patients of younger age, with emmetropia or low myopia, thicker choroids, choroidal vascular hyperpermeability on ICGA, chrysanthemum lesions, and a higher frequency of FCE and subretinal fibrosis. These clinical and MMI characteristics of cluster 2 include those seen in the pachychoroid disease spectrum, leading us to propose a new subtype of PIC called "punctate inner pachychoroidopathy."

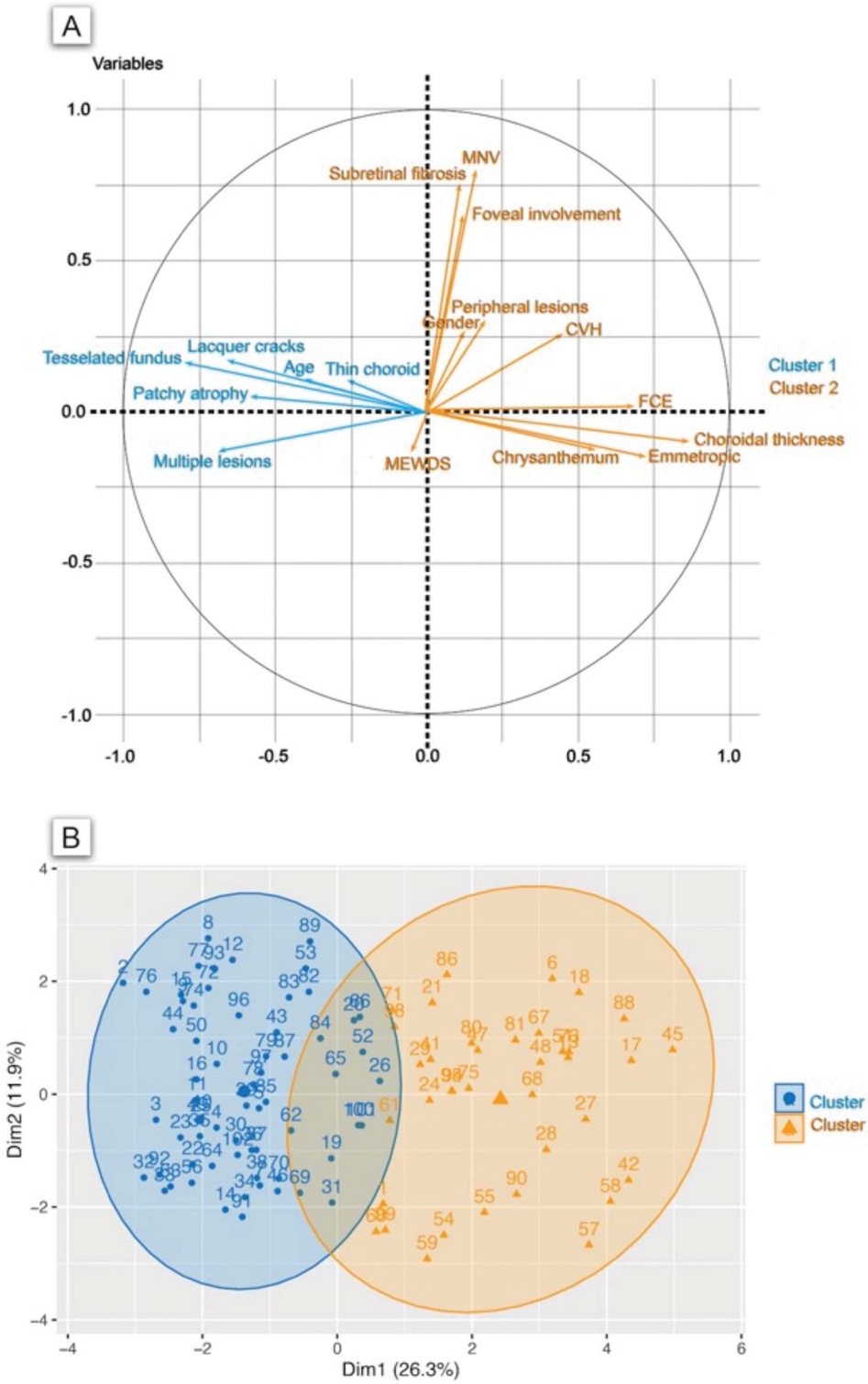

Fig. 1. Unsupervised machine learning cluster analysis of patients with PIC. **A.** In the correlation plot, positively correlated variables are shown as arrows in the same circle quadrants, and negatively correlated variables are grouped on the opposite quadrants. The length of each arrow corresponds to the squared coordinates (cosine squared, cos^2) and is proportional to the variable representation on the principal component. **B.** Scatter plot showing the results of the unsupervised machine learning clustering. The scatter plot indicates the position of each patient according to the similarity by dimensionality reduction. Patients are divided into cluster 1 (blue dots, n = 65 eyes) and cluster 2 (orange dots, n = 37 eyes). CVH, choroidal vascular hyperpermeability.

The clinical and MMI features of patients in the first cluster were consistent with the original descriptions of PIC in highly myopic patients.[2] Our results also confirm that PIC lesions may contribute to the development of patchy chorioretinal atrophy in highly myopic eyes (Figure 2).[7] Conversely, PIC lesions have never been explicitly described in eyes with pachychoroid disease. Although the mean choroidal thickness

Table 2. Demographic and Clinical Characteristics of all Patients with PIC According to Clusters

	Cluster 1 (N = 65 Eyes)	Cluster 2 (N = 37 Eyes)	*P*
Age (years)			
Mean (SD)	45.5 (13.6)	35.8 (11.7)	0.02*
Median [min, max]	44.0 [21.0, 77.0]	34.0 [14.0, 62.0]	
Sex			
Female	52 (80.0%)	29 (78.4%)	0.5
Male	13 (20.0%)	8 (21.6%)	
Refraction (diopters)			
Mean (SD)	−10.5 (4.35)	−3.89 (4.12)	0.02*
Median [min, max]	−10.4 [−23.0, −2.50]	−4.00 [−13.5, 2.50]	
Tessellated fundus			
No	3 (4.6%)	30 (81.1%)	<0.001*
Yes	62 (95.4%)	7 (18.9%)	
Lacquer cracks			
No	25 (38.5%)	36 (97.3%)	0.01*
Yes	40 (61.5%)	1 (2.7%)	
Number of lesions			
Single	12 (18.5%)	29 (78.4%)	0.04*
Multiple	53 (81.5%)	8 (21.6%)	
Peripheral lesions			
No	52 (80.0%)	28 (75.7%)	0.7
Yes	13 (20.0%)	9 (24.3%)	
Foveal involvement			
No	29 (44.6%)	12 (32.4%)	0.4
Yes	36 (55.4%)	25 (67.6%)	
SCT (μm)			
Mean (SD)	120 (65.1)	281 (81.2)	<0.001*
Median [min, max]	110 [23.0, 300]	277 [110, 470]	
MNV			
No	26 (40.0%)	12 (32.4%)	0.5
Yes	39 (60.0%)	25 (67.6%)	
FCE			
No	65 (100%)	18 (48.6%)	N/A
Yes	0 (0%)	19 (51.4%)	
Chrysanthemum lesion			
No	64 (98.5%)	23 (62.2%)	<0.001*
Yes	1 (1.5%)	14 (37.8%)	
Secondary MEWDS			
No	47 (72.3%)	27 (73.0%)	0.9
Yes	18 (27.7%)	10 (27.0%)	
Choroidal vascular hyperpermeability			
No	57 (87.7%)	21 (56.8%)	<0.001*
Yes	8 (12.3%)	16 (43.2%)	
Subretinal fibrosis			
No	43 (66.2%)	19 (51.4%)	0.3
Yes	22 (33.8%)	18 (48.6%)	
Patchy chorioretinal atrophy after PIC lesion regression			
No	14 (21.5%)	27 (73.0%)	0.04*
Yes	51 (78.5%)	10 (27.0%)	
Choroidal thinning after PIC lesion regression			
No	43 (66.2%)	31 (83.8%)	0.1
Yes	22 (33.8%)	6 (16.2%)	

*Statistically significant.
N/A, not assessed.

in patients of cluster 2 (i.e., punctate inner pachychoroidopathy) was <300 μm, it was significantly higher than of those in cluster 1 and may exceed the choroidal thickness expected in a data set of myopic eyes.[19] In addition, the prevalence of choroidal vascular hyperpermeability, which is an ICGA signature of choroidal

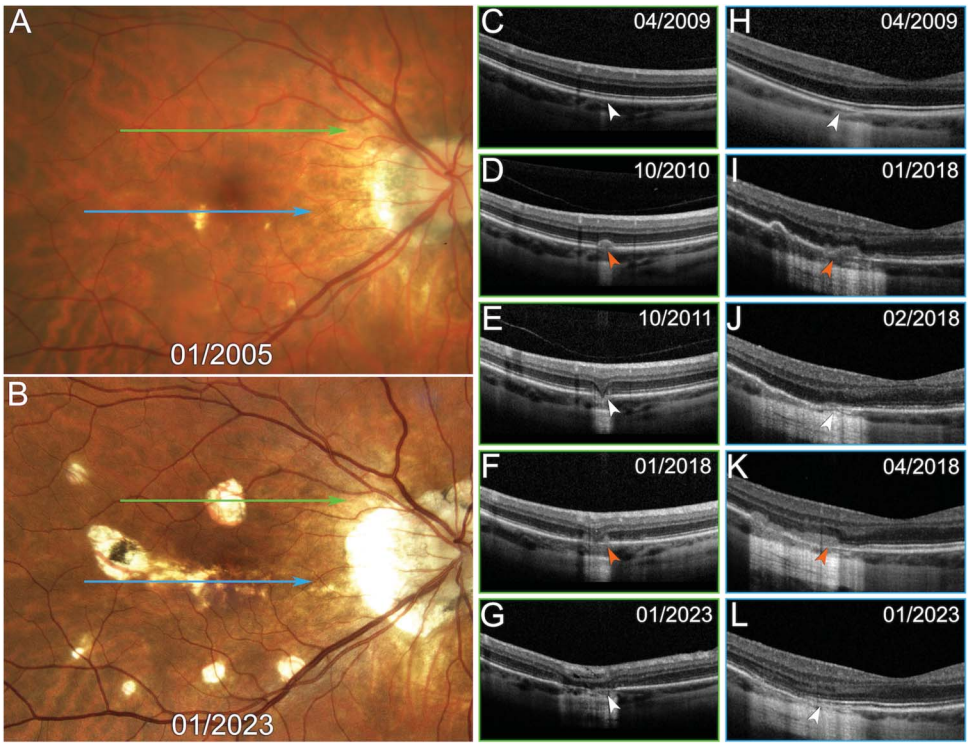

Fig. 2. Representative case of PIC associated with myopic maculopathy (cluster 1) and patchy chorioretinal atrophy development. **A.** Color fundus photography of the right eye of a myopic female patient in her 40s (refractive error: −10.00 diopters) shows myopic maculopathy features, including tessellated fundus and patchy chorioretinal atrophy in the macula and peripapillary area. The green and blue lines indicate the location of the OCT B scans displayed in (**C–G**) and (**H–L**), respectively. The time point is displayed. **B.** At the 18-year follow-up, confocal color fundus photography shows new-onset patchy chorioretinal atrophy and enlargement of preexistent atrophic areas in the macula. The green and blue lines indicate the location of the OCT B scans displayed in (**C–G**) and (**H–L**), respectively. The time point is displayed. **C–G.** Tracked OCT B scans through the superior macula (*green lines* in **A** and **B**) show the natural course of patchy chorioretinal atrophy development in myopic maculopathy. Note the absence of RPE and outer retinal atrophy at baseline (*white arrowhead* in **C**). Development and enlargement of patchy chorioretinal atrophy (*white arrowheads* in **E** and **G**) are preceded by recurrent episodes of PIC lesions (*orange arrowheads* in **D** and **F**) characterized by subretinal isoreflective material splitting the RPE/BrM complex. The time points are displayed. **H–L.** Tracked OCT B scans through the fovea (*blue lines* in **A** and **B**) show the natural course of patchy chorioretinal atrophy development in myopic maculopathy. Note the subtle posterior signal hypertransmission indicative of RPE/BrM complex alteration at baseline (*white arrowhead* in **H**). Development and enlargement of patchy chorioretinal atrophy (*white arrowheads* in **J** and **L**) are preceded by recurrent episodes of PIC lesions (*orange arrowheads* in **I** and **K**) characterized by subretinal isoreflective material splitting the RPE/BrM complex. The time points are displayed. Note the asynchronism of PIC lesions in different macular locations.

venous congestion or insufficiency,[20] significantly differed between the two clusters. This observation supports that PIC can occur in eyes with a preexistent choroidal venous insufficiency. While the Standardization of Uveitis Nomenclature Working Group defined PIC as a multifocal disease,[21] our study demonstrated that most patients displaying pachychoroid disease featured a singular lesion. Our results align with a recent study that outlined the occurrence of solitary lesions within the spectrum of PIC.[22]

Choroidal venous insufficiency may play a role in the pathogenesis of FCE.[23] Venous insufficiency may create a proinflammatory environment or cause defective clearance of inflammatory cells and cytokines, eliciting local inflammation.[24] The effect of venous hypertension on the state of leukocyte activation has been investigated in patients with lower extremity venous insufficiency.[24] Leucocytes "trapped" into the circulation of legs during venous hypertension acquire an activated profile. Histologic studies of the skin in patients with chronic venous disease showed perivascular infiltration of the capillaries of the most superficial part of the dermis with monocytes, macrophages, and connective tissue proteins, including fibrin.[25] Hence, we hypothesized that choroidal venous insufficiency may predispose to local inflammation, clinically presenting as PIC.

Focal choroidal excavation can occur in pachychoroid disease spectrum, inherited retinal dystrophies, or inflammatory chorioretinal diseases.[26] In these patients, FCE is believed to derive from BrM defects and choroidal scarring, atrophy, and contraction at the site of a previous traumatic, degenerative, or inflammatory process.[27] Focal choroidal excavation can complicate up to 20% of eyes with PIC lesions.[28] In our series, FCE was found in 100% of cluster 2 patients and none in cluster 1, suggesting that pachychoroid disease features are a prerequisite to FCE formation. In eyes with PIC lesions, focal inflammatory infiltration of the inner choroid and disruption of the RPE/BrM complex may be initiating or exacerbating factors for FCE development. In our series, some patients with FCE showed no signs of chorioretinal inflammation at the first visit and only developed

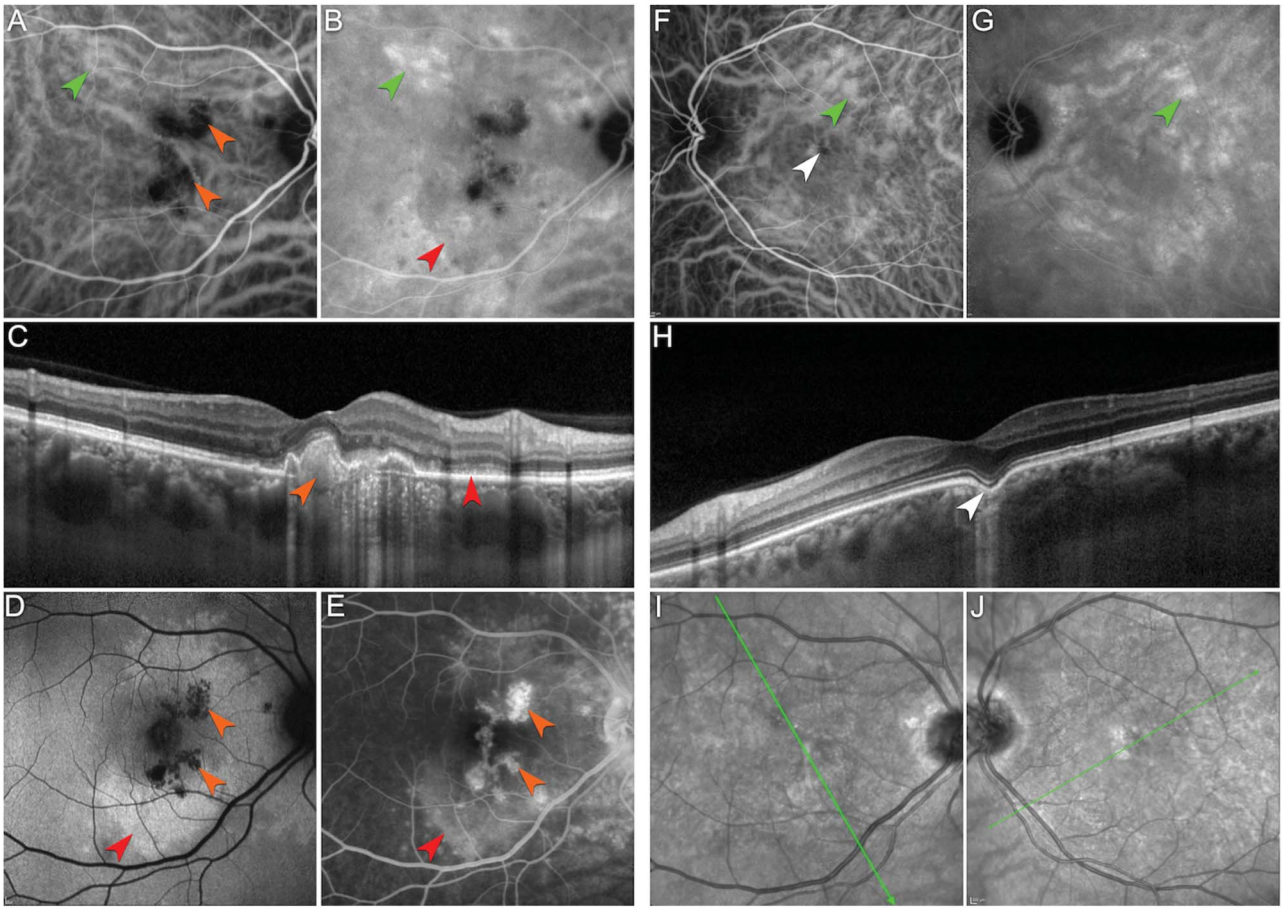

Fig. 3. A representative case of punctate inner pachychoroidopathy (cluster 2) with chrysanthemum lesions and secondary MEWDS. **A.** Early phase of ICGA of the right eye shows multiple hypofluorescent lesions consistent with PIC (*orange arrowheads*). Note the dilated choroidal veins in the superior macula (*green arrowhead*). **B.** Late-phase ICGA of the right eye shows multiple areas of choroidal vascular hyperpermeability (*green arrowhead*). Note the late hypofluorescence surrounding the PIC lesions (*red arrowhead*) suggestive of secondary MEWDS (*reduced retinal pigment epithelium uptake*). **C.** Optical coherence tomography (OCT) B scan shows a subretinal hyperreflective material splitting the RPE/BrM complex and associated with posterior signal hypertransmission and loss of the normal choroidal architecture (*orange arrowhead*). Note the diffuse increased choroidal thickness in the macula with pachyvessels compressing the inner choroid. The ellipsoid zone and interdigitation zone in the vicinity of the PIC lesions are disrupted (*red arrowhead*), which suggests secondary MEWDS. **D.** Fundus autofluorescence imaging of the right eye shows multiple hypoautofluorescent chrysanthemum lesions (*orange arrowheads*). Note the area of hyperautofluorescence surrounding the PIC lesions (*red arrowhead*) and suggestive of secondary MEWDS. **E.** Midphase fluorescein angiography of the right eye shows hyperfluorescent chrysanthemum lesions (*orange arrowheads*). Note the area of hyperfluorescence surrounding the PIC lesions (*red arrowhead*) suggestive of secondary MEWDS. **F.** Early-phase ICGA of the left eye shows a discrete hypofluorescent lesion in the fovea (*white arrowhead*). Note the dilated choroidal veins in the superior macula (*green arrowhead*). **G.** Late-phase ICGA of the left eye shows multiple areas of choroidal vascular hyperpermeability (*green arrowhead*). **H.** OCT B scan through the fovea shows a focal choroidal excavation (*white arrowhead*). **I.** Near-infrared reflectance image of the right eye with the green line indicating the location of the OCT B scan displayed in (**C**). **J.** Near-infrared reflectance image of the left eye with the green line indicating the location of the OCT B scan displayed in **H**.

PIC lesions during the follow-up period (from months to years) (Figure 5). In these patients, FCE may be erroneously diagnosed as idiopathic or secondary to noninflammatory conditions. Moreover, several authors have reported MNV associated with idiopathic FCE, advocating choroidal hypoperfusion, RPE stretching, and RPE/BrM damage as eliciting factors.[29] We suspect some of these MNV cases were inflammatory and developed at the site of a previous asymptomatic or subclinical PIC lesion. We advocate scrutinizing multimodal imaging for signs suggestive of PIC because prompt recognition and treatment are essential to avoid irreversible damage related to disease relapse. Long-term follow-up may also be warranted to detect active PIC lesions and MNV in eyes with FCE.[30]

Interestingly, we found no significant difference in the occurrence of secondary MEWDS between the two clusters. This may suggest that the pathogenesis of secondary MEWDS is not influenced by choroidal venous insufficiency. Secondary MEWDS has been described in the course of active PIC lesions, and disruption of the RPE/BrM and loss of the subretinal immune privilege have been suggested as promoting

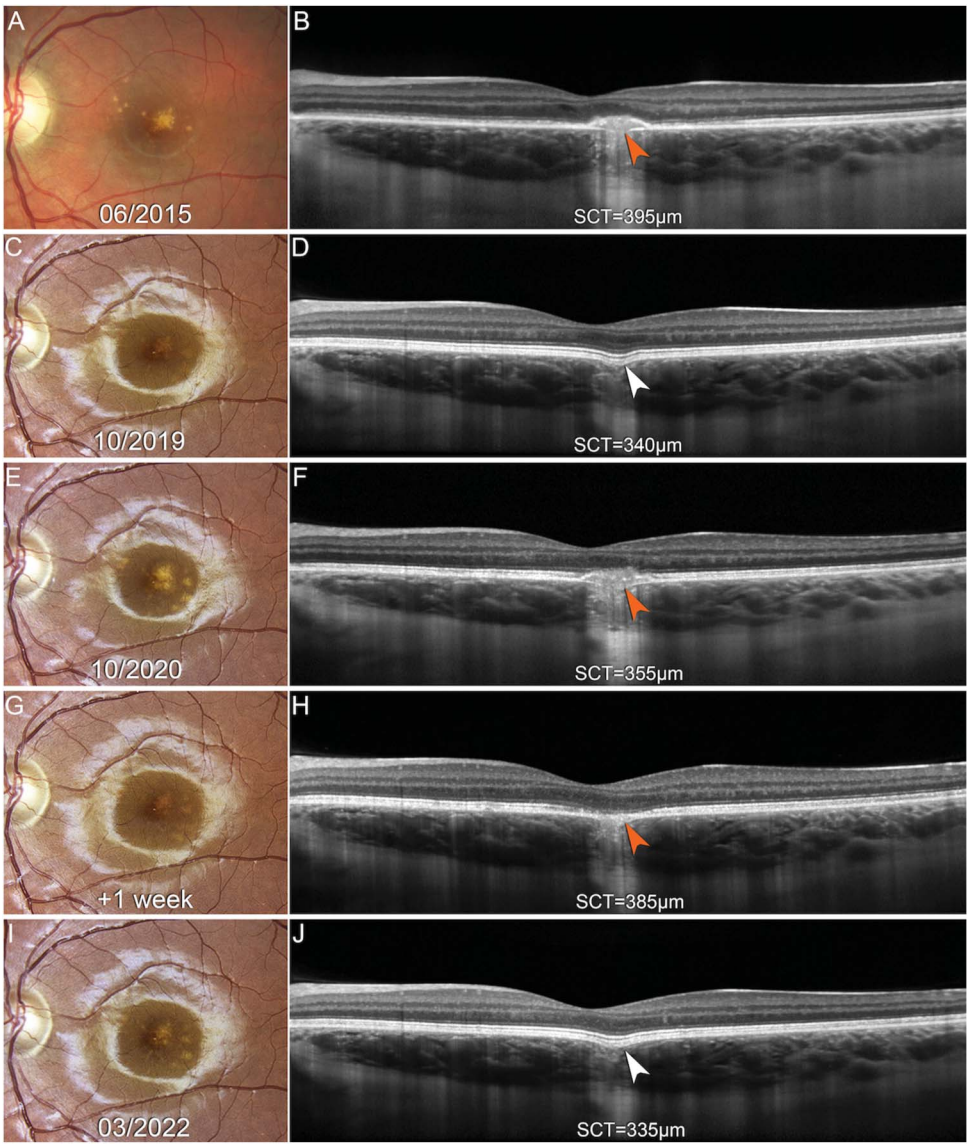

Fig. 4. Representative case of punctate inner pachychoroidopathy (cluster 2) and focal choroidal excavation formation. **A.** Color fundus photography of the left eye of a myopic female patient in her 20s (refractive error: −3.00 diopters) shows a chrysanthemum lesion characterized by a gray-yellow central lesion surrounded by satellite pale dots. Note the reduced fundus tessellation suggestive of increased choroidal thickness and the absence of myopic maculopathy features. The time point is displayed. **B.** Corresponding horizontal OCT B scan through the fovea shows a subretinal hyperreflective material splitting the RPE/BrM complex and associated with posterior signal hypertransmission and loss of the normal choroidal architecture (*orange arrowhead*). Note the diffuse increased choroidal thickness in the macula with pachyvessels compressing the inner choroid. The ellipsoid zone and interdigitation zone in the vicinity of the PIC lesion are disrupted, which suggests secondary MEWDS. The SCT is noted. **C.** At the 4-year follow-up, confocal color fundus photography shows hypopigmentary changes in the macula. The time point is displayed. **D.** Corresponding horizontal OCT B scan through the fovea shows a focal choroidal excavation (*white arrowhead*) at the site of the previous PIC lesion. Note the restoration of the ellipsoid zone/interdigitation zone bands in the macula. The SCT is noted. **E.** At the 5-year follow-up, confocal color fundus photography shows a recurrent chrysanthemum lesion in the macula. The time point is displayed. **F.** Corresponding horizontal OCT B scan through the fovea shows a recurrence of subretinal hyperreflective material splitting the RPE/BrM complex and associated with posterior signal hypertransmission and loss of the normal choroidal architecture (*orange arrowhead*). The SCT is noted. **G.** One week after the recurrent PIC lesion and under oral corticosteroid (1 mg/kg/day), confocal color fundus photography shows progressive healing of the PIC lesion. The time point is displayed. **H.** Corresponding horizontal OCT B scan through the fovea shows a reduction of the inflammatory hyperreflective material splitting the RPE/BrM complex (*orange arrowhead*). Note the paradoxical increased choroidal thickness under oral corticosteroid. The SCT is noted. **I.** At the 7-year follow-up, confocal color fundus photography shows residual hypopigmentary changes in the macula. The time point is displayed. **J.** Corresponding horizontal OCT B scan through the fovea shows a focal choroidal excavation (*white arrowhead*). The SCT is noted.

factors.[4–6] Secondary MEWDS usually starts in the vicinity of PIC lesions and shows secondary centrifugal spreading. Subsequent incremental amplification of the photoreceptor inner and outer segment-specific insult may account for the extension of the hyperautofluorescent spots and the ellipsoid zone/interdigitation zone disruption on fundus autofluorescence imaging and OCT imaging, respectively.[11]

Regarding treatment, corticosteroids have shown efficacy in controlling active PIC lesions.[31] However, the presence of inflammatory chorioretinal conditions in eyes with preexisting pachychoroid disease features presents a challenge in therapeutic drug selection and monitoring. Corticosteroid usage is a risk factor of central serous chorioretinopathy, and it may precipitate fluid drainage imbalance in eyes with pachychoroid disease features. In our series, all eyes presenting with active PIC lesions were treated with systemic or local corticosteroids and showed positive responses without subretinal fluid accumulation. Owing to the prompt resolution of active PIC lesions in eyes with pachychoroid disease features, we believe that there is a

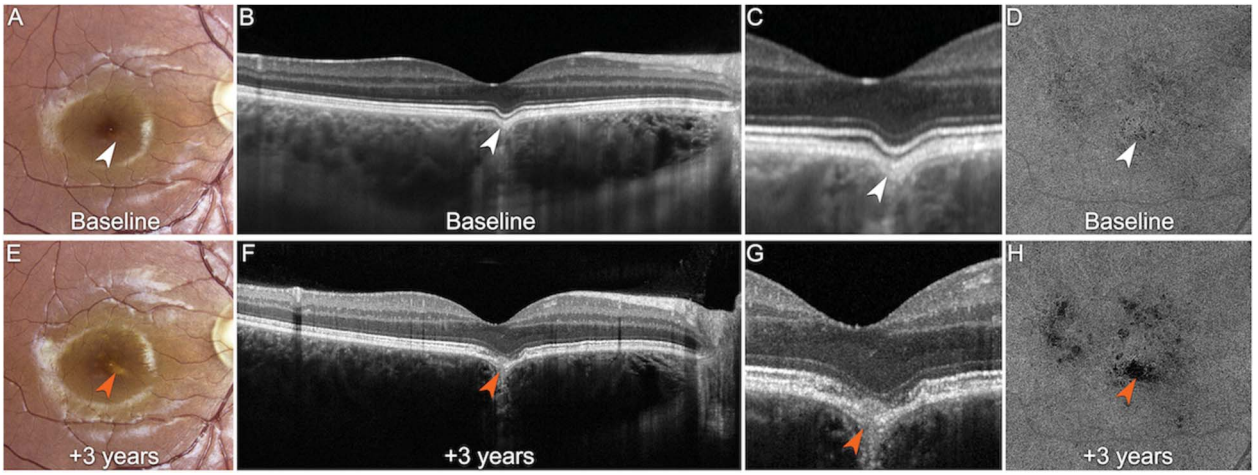

Fig. 5. Punctate inner pachychoroidopathy (cluster 2) associated with preexistent focal choroidal excavation and pachychoroid disease features. **A.** At baseline, confocal color fundus photography of the right eye shows subtle hypopigmented changes of the RPE in the fovea (*white arrowhead*). The time point is displayed. **B.** Corresponding horizontal SD-OCT B scan through the fovea shows a focal choroidal excavation (*white arrowhead*). Note the diffuse increased choroidal thickness in the macula with pachyvessels compressing the inner choroid. The time point is displayed. **C.** Magnified view of the focal choroidal excavation on SD-OCT (*white arrowhead*). Note the continuity of the ellipsoid zone. **D.** En face SS-OCTA segmented at the level of the choriocapillaris shows subtle flow signal deficits (*white arrowhead*) colocalizing with the focal choroidal excavation. The time point is displayed. **E.** At the 3-year follow-up, confocal color fundus photography of the right eye shows a PIC lesion (*orange arrowhead*). The time point is displayed. **F.** Corresponding horizontal high-resolution SD-OCT (High-Res OCT) B scan through the fovea shows a discrete subretinal hyperreflective material splitting the RPE/BrM complex at the site of the focal choroidal excavation (*orange arrowhead*). Note the posterior signal hypertransmission. The time point is displayed. **G.** Magnified view of the PIC lesion colocalizing with the focal choroidal excavation on High-Res OCT (*orange arrowhead*). Note the disruption of the ellipsoid zone band and the focal RPE/BrM complex interruption. **H.** En face SS-OCTA segmented at the level of the choriocapillaris shows an enlargement of the flow signal deficits colocalizing with the PIC lesion (*orange arrowhead*). The time point is displayed. SS-OCTA, swept-source OCT angiography

definite benefit in treating these patients with corticosteroids when indicated. Moreover, reduced choroidal thickness, often regarded as a sign of resolved choroidal inflammation,[2] may not be a suitable indicator of treatment response in patients with punctate inner pachychoroidopathy.

The strengths of this study are the relatively large sample size and advanced statistical analysis. Limitations include the retrospective nature, incomplete MMI data in some cases, and lack of standardized follow-up. The k-means clustering algorithm also has potential limitations. First, it assumes prior knowledge of the data and the appropriate number of clusters. Second, the results obtained are sensitive to the initial random selection of cluster centers, which may lead to different clustering results on different algorithm runs. Finally, it is susceptible to outliers and data ordering.

In summary, phenotypic cluster analyses suggested two PIC subtypes defined principally by the presence or absence of pachychoroid disease features. A preexistent choroidal venous insufficiency may influence the disease manifestations, treatment responses, and complications. Identification of active PIC lesions in eyes with pachychoroid disease features may provide a reappraisal of the pathophysiologic background of FCE in the pachychoroid disease spectrum.

Key words: punctate inner choroidopathy, pachychoroid, choroidal venous congestion, white spot syndromes, cluster analysis.

Acknowledgments

K. B. Freund is a consultant for Heidelberg Engineering, Zeiss, Allergan, Bayer, Genentech, and Novartis and receives research support from Genentech/Roche. F. Bandello is a consultant for Allergan Inc (Irvine, CA), Bayer Shering-Pharma (Berlin, Germany), Hoffmann-La-Roche (Basel, Switzerland), Novartis (Basel, Switzerland), Sanofi-Aventis (Paris, France), Thrombogenics (Heverlee, Belgium), Zeiss (Dublin, OH), Boehringer-Ingelheim, Fidia Sooft, Ntc Pharma, and Sifi. The other authors report no disclosures. Other acknowledgments such as statisticians, medical writers, and expert contributions: There are no other acknowledgments.

References

1. Essex RW, Wong J, Jampol LM, et al. Idiopathic multifocal choroiditis: a comment on present and past nomenclature. Retina 2013;33:1–4.
2. Spaide RF, Goldberg N, Freund KB. Redefining multifocal choroiditis and panuveitis and punctate inner choroidopathy through multimodal imaging. Retina 2013;33:1315–1324.

3. Vance SK, Khan S, Klancnik JM, Freund KB. Characteristic spectral-domain optical coherence tomography findings of multifocal choroiditis. Retina 2011;31:717–723.
4. Cicinelli MV, Hassan OM, Gill MK, et al. A multiple evanescent white dot syndrome-like reaction to concurrent retinal insults. Ophthalmol Retina 2021;5:1017–1026.
5. Essilfie J, Bacci T, Abdelhakim AH, et al. Are there two forms of multiple evanescent white dot syndrome? Retina 2022;42: 227–235.
6. Ramtohul P, Cabral D, Cicinelli MV, Freund KB. Recurrence of acute retinopathy in pseudoxanthoma elasticum. Retinal Cases Brief Rep 2022. Epub ahead of print.
7. Hady SK, Xie S, Freund KB, et al. Prevalence and characteristics of multifocal choroiditis/punctate inner choroidopathy in pathologic myopia eyes with patchy atrophy. Retina 2022;42:669–678.
8. Cheung CMG, Lee WK, Koizumi H, et al. Pachychoroid disease. Eye (Lond) 2019;33:14–33.
9. Ramtohul P, Cabral D, Oh D, et al. En face ultrawidefield OCT of the vortex vein system in central serous chorioretinopathy. Ophthalmol Retina 2023;7:346–353.
10. Chung H, Byeon SH, Freund KB. Focal choroidal excavation and its association with pachychoroid spectrum disorders: a review of the literature and multimodal imaging findings. Retina 2017;37:199–221.
11. Abdelhakim AH, Yannuzzi LA, Freund KB, Jung JJ. Differential response to glucocorticoid immunosuppression of two distinct inflammatory signs associated with punctate inner choroidopathy. Retina 2021;41:812–821.
12. Cicinelli MV, Marchese A, Ramtohul P, et al. Punctate inner choroidopathy-like reactions in unrelated retinal diseases. Retina 2022;42:2099–2109.
13. Du R, Fang Y, Jonas JB, et al. Clinical features of patchy chorioretinal atrophy in pathologic myopia. Retina 2020;40:951–959.
14. Ramtohul P, Malcles A, Gigon E, et al. Long-term outcomes of bacillary layer detachment in neovascular age-related macular degeneration. Ophthalmol Retina 2022;6:185–195.
15. Ramtohul P, Cicinelli MV, Dolz-Marco R, et al. The chrysanthemum phenotype of idiopathic multifocal choroiditis. Retina 2023;43:1377–1385.
16. Spaide RF, Yannuzzi LA, Freund KB. Linear streaks in multifocal choroiditis and panuveitis. Retina 1991;11:229–231.
17. Ohno-Matsui K, Kawasaki R, Jonas JB, et al. International photographic classification and grading system for myopic maculopathy. Am J Ophthalmol 2015;159:877–883.e7.
18. Lê S, Josse J, FactoMineR HussonF. A package for multivariate analysis. J Stat Softw 2008;25:1–18.
19. Flores-Moreno I, Lugo F, Duker JS, Ruiz-Moreno JM. The relationship between axial length and choroidal thickness in eyes with high myopia. Am J Ophthalmol 2013;155:314–319.e1.
20. Bacci T, Oh DJ, Singer M, et al. Ultra-widefield indocyanine green angiography reveals patterns of choroidal venous insufficiency influencing pachychoroid disease. Invest Ophthalmol Vis Sci 2022;63:17.
21. Standardization of Uveitis Nomenclature SUN Working Group. Classification criteria for punctate inner choroiditis. Am J Ophthalmol 2021;228:275–280.
22. Gan Y, He G, Zeng Y, et al. Solitary punctate chorioretinitis—a unique subtype of punctate inner choroidopathy. Retina 2023;43:1487–1495.
23. Ramtohul P, Engelbert M, Malcles A, et al. Bacillary layer detachment: multimodal imaging and histologic evidence of a novel optical coherence tomography terminology: literature review and proposed theory. Retina 2021;41:2193–2207.
24. Smith PD. Neutrophil activation and mediators of inflammation in chronic venous insufficiency. J Vasc Res 1999;36:24–36.
25. Coleridge Smith PD. Update on chronic-venous-insufficiency-induced inflammatory processes. Angiology 2001;52:S35–S42.
26. Battaglia Parodi M, Casalino G, Iacono P, et al. The expanding clinical spectrum of choroidal excavation in macular dystrophies. Retina 2018;38:2030–2034.
27. Gan Y, Ji Y, Zuo C, et al. Correlation between focal choroidal excavation and underlying retinochoroidal disease: a pathological hypothesis from clinical observation. Retina 2022;42:348–356.
28. Kim H, Woo SJ, Kim YK, et al. Focal choroidal excavation in multifocal choroiditis and punctate inner choroidopathy. Ophthalmology 2015;122:1534–1535.
29. Xu H, Zeng F, Shi D, et al. Focal choroidal excavation complicated by choroidal neovascularization. Ophthalmology 2014;121:246–250.
30. Orellana-Rios J, Leong BCS, Fernandez-Avellaneda P, et al. Late recurrence of choroidal neovascularization in patients with multifocal choroiditis: clinical surveillance in perpetuity. Retinal Cases Brief Rep 2022;16:233–241.
31. Ahnood D, Madhusudhan S, Tsaloumas MD, et al. Punctate inner choroidopathy: a review. Surv Ophthalmol 2017;62:113–126.